

Supplementary Information for

Mutational landscape of primary, metastatic and recurrent ovarian cancer reveals c-MYC gains as potential target for BET inhibitors

Charles Li^{a,1}, Elena Bonazzoli^{b,1}, Stefania Bellone^b, Jungmin Choi^a, Weilai Dong^a, Gulden Menderes^b, Gary Altwenger^b, Chanhee Han^b, Aranzazu Manzano^b, Anna Bianchi^b, Francesca Pettinella^b, Paola Manara^b, Salvatore Lopez^b, Ghanshyam Yadav^b, Francesco Riccio^b, Luca Zammataro^b, Burak Zeybek^b, Yang Yang-Hartwich^b, Natalia Buza^c, Pei Hui^c, Serena Wong^c, Antonella Ravaggi^d, Eliana Bignotti^d, Chiara Romani^d, Paola Todeschini^d, Laura Zanotti^d, Valentina Zizioli^d, Franco Odicino^d, Sergio Pecorelli^d, Laura Ardighieri^e, Dan-Arin Silasi^b, Babak Litkouhi^b, Elena Ratner^b, Masoud Azodi^b, Gloria S. Huang^b, Peter E. Schwartz^b, Richard P. Lifton^f, Joseph Schlessinger^{g,2}, and Alessandro D. Santin^b

Joseph Schlessinger

Email: joseph.schlessinger@yale.edu

This PDF file includes:

Supplementary text

Figs. S1 to S7

Tables S1 to S10

References for SI reference citations

Supplementary Information Text

Materials and Methods

Patients and specimens. The study protocol was approved by the Yale Human Investigation Committee. Prior to surgical staging, patients were consented for tumor banking in accordance with the Declaration of Helsinki. DNA was extracted from 90 primary tumors, including 13 matched pairs from patients with bilateral ovarian tumors, metastatic tumors (n=41), and recurrent tumors (n=17) who underwent surgical staging for the treatment for their disease at Yale University, New Haven, CT or the University of Brescia School of Medicine, Brescia, Italy. The majority of the tumors had high grade serous ovarian cancer (HG-SOC) histology (Table S1). The 1988 FIGO staging system was used and histology was further evaluated by board-certified pathologists to confirm that the frozen section was histologically consistent with an ovarian carcinoma. Main criteria for selection were: 1) the diagnosis of ovarian cancer confirmed by the review of a minimum of 2 Board certified surgical pathologists with specific expertise in Gynecologic oncology, 2) the availability for light microscopic evaluation of a hematoxylin and eosin stained section of each frozen tumor specimen submitted to sequencing for assessment of percent tumor nuclei and percent necrosis in addition to other pathology annotations and 3) the availability of sufficient fresh frozen tumor tissue for DNA extraction for NGS. Genomic DNA was prepared from venous blood, primary fibroblast cultures or frozen myometrium by standard procedures. We confirmed that each section contains a high purity of tumor (>40%) and minimal necrosis and used those sections for DNA extraction. Primary ovarian cancer cell lines with tumor purity above 90% and less than 3 weeks of culture in vitro were used for sequencing. We also performed whole-exome sequencing on DNA extracted from 13 matched ovarian cancer pairs (ie, right and left ovarian cancers) from patients with bilateral tumors.

Whole exome sequencing. For fresh frozen and cell line samples, genomic DNA was isolated by Allprep DNA kit (Qiagen # 80204). For FFPE samples, DNA was extracted by BiOstic® FFPE Tissue DNA Isolation Kit (MO BIO Laboratories #12250-50) with a modified protocol.

Genomic DNA was captured on the NimbleGen 2.1M human exome array and subjected to 74 base paired-end reads on the Illumina HiSeq 2000 instrument as described (1). Sequence reads were mapped to the reference genome (hg19) using the ELAND program. Reads outside the targeted sequences were discarded and statistics on coverage were collected from the remaining reads using in-house Perl scripts.

Somatic point mutation and indel calling. For matched normal-tumor pairs, somatic point mutations were called by MuTect2. The output was further filtered to remove false positives caused by low base/read quality or mismapping. We also required a minimum number of reads with non-reference alleles based on total coverage of the position and sequencing error of the platform. Somatic indels were called by an in-house pipeline detecting regions with multiple nearby loci showing differences of reference and non-reference reads coverage between tumor and normal samples. All indels have been manually curated. For unmatched tumors, SAMtools was used to call variant bases appended with quality scores. Among these, variants with frequency more than 2×10^{-5} in

ExAC (Exome Aggregation Consortium (ExAC), Cambridge, MA (URL: <http://exac.broadinstitute.org>) were excluded and the rest were considered as potential somatic variants. Identified variants were annotated based on novelty, impact on the encoded protein, conservation, and expression using an automated pipeline.

Somatic copy number mutation calling. Copy number variants were identified by comparing coverage depth of individual capture intervals (0.5Mb bins) from primary, metastatic and recurrent tumor and normal samples after normalization for mean coverage depth of each exome. A permutation-based strategy was used to assess the significance of recurrent CNVs with a false discovery rate cutoff of 0.25 after Benjamini Hochberg correction previously detailed in (2). LOH calling and purity estimation were performed as previously described (2). Independent significant CNV peaks were called based on a GISTIC-like peel algorithm (3).

Evaluation of subclonality in SBOC samples. Variant allele fraction of somatic mutations called by MuTect2 and allele-specific copy number variations called by Sequenza (4) were provided to PyClone (5) to cluster cancer cell fractions using a hierarchical Bayesian clustering model. Clusters containing at least two mutations were used to infer a consensus clonal evolution model for bilateral ovarian tumors using ClonEvol (6).

Real-time reverse transcription-PCR (qRT-PCR). RNA isolation from carcinoma cell lines and fresh frozen tissues was performed using AllPrep DNA/RNA/Protein Mini Kit (Qiagen, Valencia, CA, USA), according to the manufacturer's instructions. Quantitative PCR was carried out with a 7500 RealTime PCR System using the manufacturer's recommended protocol (Applied Biosystems, Foster City, CA, USA) to evaluate the expression of PIK3CA, TP53, and MYC. The primers and probes were obtained from Applied Biosystems (i.e., PIK3CA, Assay ID: Hs00180679_m1; TP53, Assay ID: Hs01034249_m1; MYC, Assay ID: Hs00153408_m1). The comparative threshold cycle method was used to determine gene expression in each sample, relative to the value observed in non-malignant endometrial epithelial cell samples collected from similar age women, using glyceraldehyde-3-phosphate dehydrogenase (Assay ID Hs99999905_m1) RNA as an internal control.

Cell lines. Primary ovarian carcinoma cell line establishment was performed as described previously from our group for uterine serous carcinomas (2). Source-patient characteristics from which sequenced tumor cell lines were established are described in Table S1.

Drug. GS-626510 and JQ1 (GS-589903) were obtained from Gilead Science. They were dissolved in DMSO (Sigma-Aldrich, St. Louis, MO) to create a 10 mM stock solution for the *in vitro* and *in vivo* studies as described below.

Cell viability assay. To determine dose-response, cells were treated with scalar amounts of each drug ranging from 0.001 μ M to 5 μ M and counted by flow cytometry as previously described (7).

Xenograft implantation and in vivo drug study. Specimen collection and all animal experiments were approved by the institutional ethical committee (HIC) and Institutional Animal Care and Use Committee (IACUC) of Yale University. Briefly, four to six week old CB-17/SCID mice were given a single subcutaneous injection of 7×10^6 KRCH31 cells in approximately 300 μ L of a 1:1 solution of sterile PBS containing cells and Matrigel (BD Biosciences) while for the PDX experiments, OMM78 was obtained from a surgical specimen at the time of a staging procedure of a high-grade serous carcinoma patient (stage IVA) and placed into a sterile Petri dish containing phosphate-buffered saline (PBS), then sliced into $5 \times 5 \times 2$ mm fragments. Typically, one fragment was implanted into a subcutaneous area in the right or left flanks in combination with Matrigel. The size of the implanted tumor was checked 1-3 times per week using Vernier calipers when the implanted tissue was palpable, and the volume was calculated as $(\text{length} \times \text{width}^2)/2$. Once the tumor volume was approximately 0.2 cm^3 for the xenografted cell lines and about 0.4 cm^3 for the PDX, the mice were randomized into treatment groups (n=5-10) and drugs delivered orally and BID for GS-626510 and IP Q-day for JQ1 (GS-589903) for a total of 21 days. On day 21, after last dose administration animals were either euthanized or follow up for overall survival as the primary outcome measure. Tumor measurements were recorded twice weekly. Mice were sacrificed if found in poor health conditions or when the tumor volume exceeded the maximum value established by the IACUC. Animal care and euthanasia were carried out according to the rules and regulations as set forth by the Institutional Animal Care and Use Committee (IACUC).

Pharmacodynamic studies in mice. Female CB17/lcrHsd-Prkd/scid mice (15-19 g) bearing KRCH31 tumors were treated orally and BID for GS-626510 and IP Q-day for JQ1 (GS-589903) and vehicle for oral gavage studies for a total of 21 days. One, 6 and 12 hours post treatment three/four animals per time point were euthanized and tumors excised and halved for analysis. One half was flash frozen and stored at -80°C for pharmacodynamics studies. The second half was fixed in formalin for 24 hours and then transferred in Ethanol 70% for biomarker and histopathological evaluation. Immunostaining results from tumor tissues excised from KRCH31 xenografted animals were interpreted using an automated computational image analysis system (Definiens Tissue Studio software, Munich, Germany). For each stain, we used the Tissue Studio software to define an intensity and size threshold for nucleus identification and to define an intensity threshold for nuclear stain positivity essentially as previously described (8). The automated analysis software was trained for scoring only the appropriate epithelial regions of the tissue. Based on these criteria, each cell was classified as positive or negative and depending on intensity of the nuclear stain, positive cells were further categorized into low-positive, medium-positive, or high-positive. For each sample, we estimated the mean percentage of stain-positive cells (at any intensity) across the cores, by weighting each core by its total cell count. Results are aggregated per animal and expressed as mean per group \pm SD. Statistical differences between experimental and control groups were measured by the two-tailed Student t-test.

Statistical analysis. The IC_{50} values of the cell lines were compared using a one-way analysis of variance. Grouped mean IC_{50} values were compared using two-tailed Student's t-test. All statistical analysis was performed using Prism 6 software (GraphPad Prism Software Inc., San Diego, CA). *P value < 0.05 was considered statistically significant.

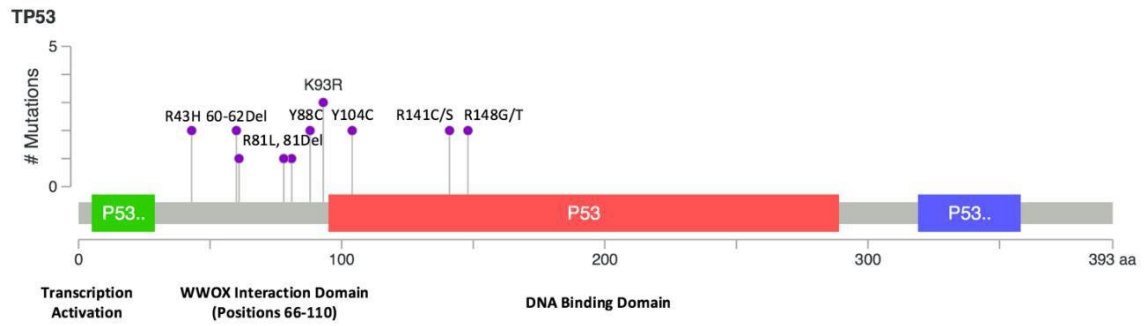


Fig. S1. Recurrent TP53 Mutations. Locations of recurrent TP53 mutation were mapped to corresponding protein domains. Mutations cluster near the WWOX (WOX1) interaction domain, a protein required for TP53 activation and apoptosis induction.

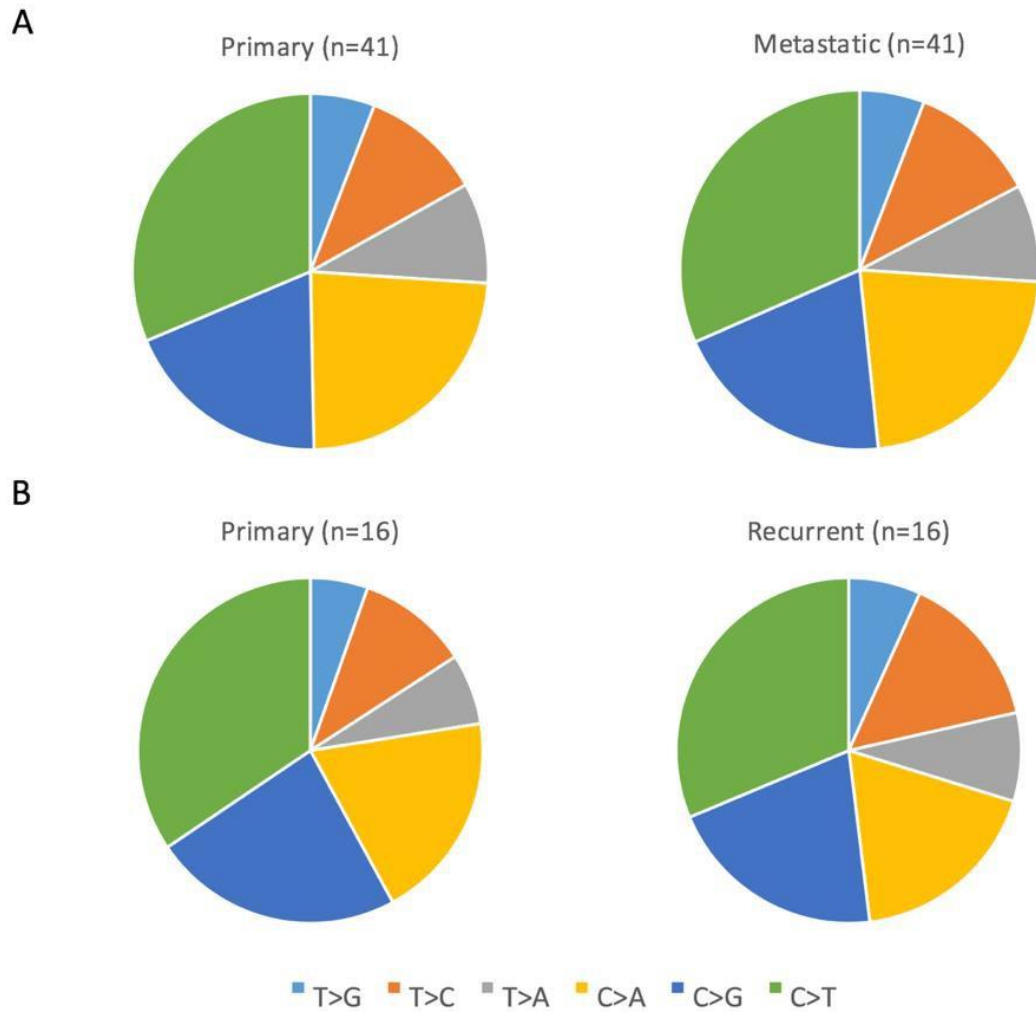


Fig. S2. Mutation Signature Analysis of Matched Tumors. Mutation signature in matched pairs of primary and metastatic tumors (A), as well as primary and recurrent tumors (B), were compared to evaluate mutation signature changes through tumor progression while controlling for differences between patients. Tumors contained nearly identical mutation signatures between primary and metastatic as well as primary and recurrent settings.

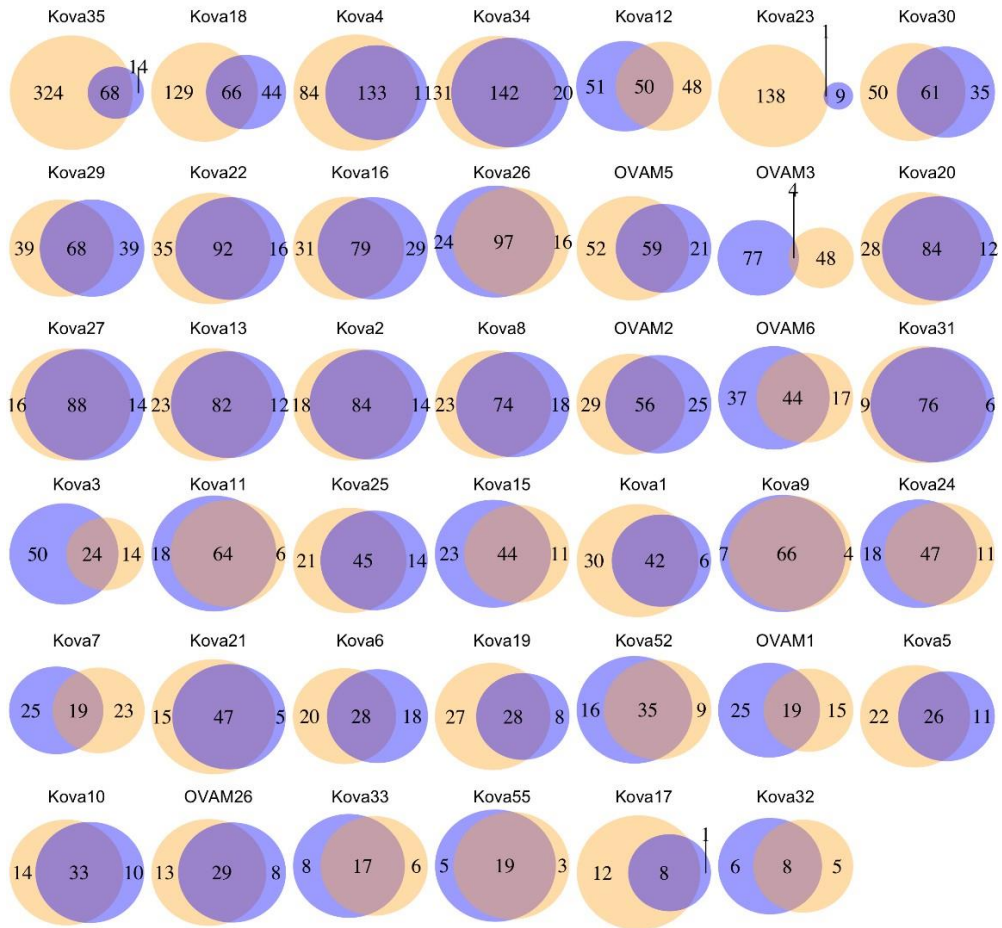


Fig. S3. Mutations in Primary and Metastatic ovarian cancers. Venn diagrams present the total number of somatic exonic mutations unique to primary/metastatic ovarian tumors or shared between the matched tumors.

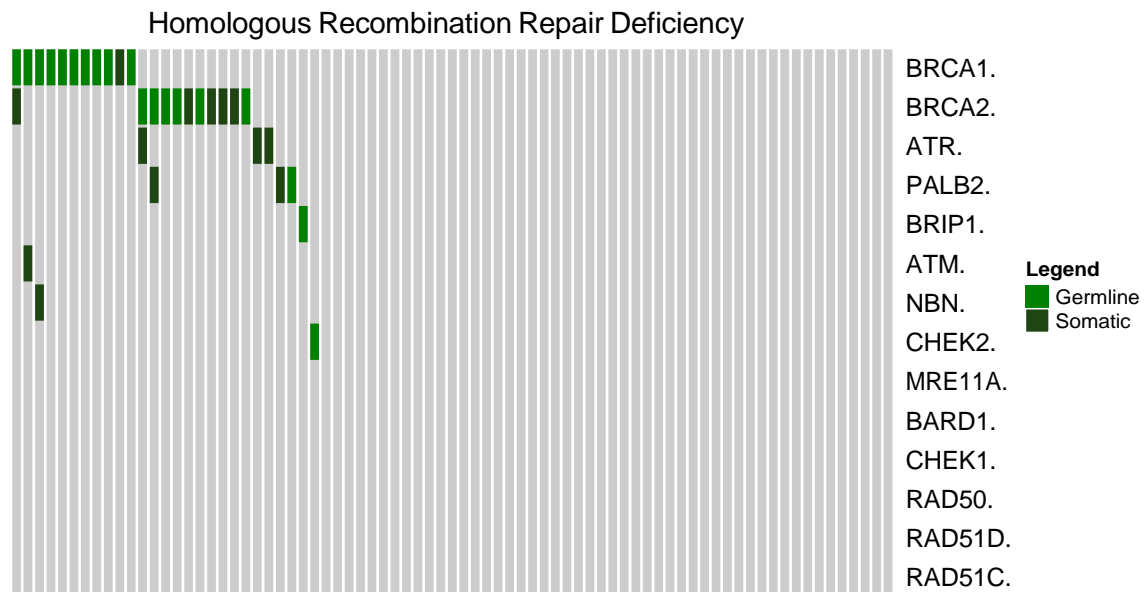


Fig. S4. Distribution of Homologous Recombination Mutations. Each patient in the cohort, represented by columns, was analyzed for known pathogenic germline mutations and indels (Light Green). Somatic mutation markers (Dark Green) indicate the presence of a somatic mutation in an HRR gene in at least one setting.

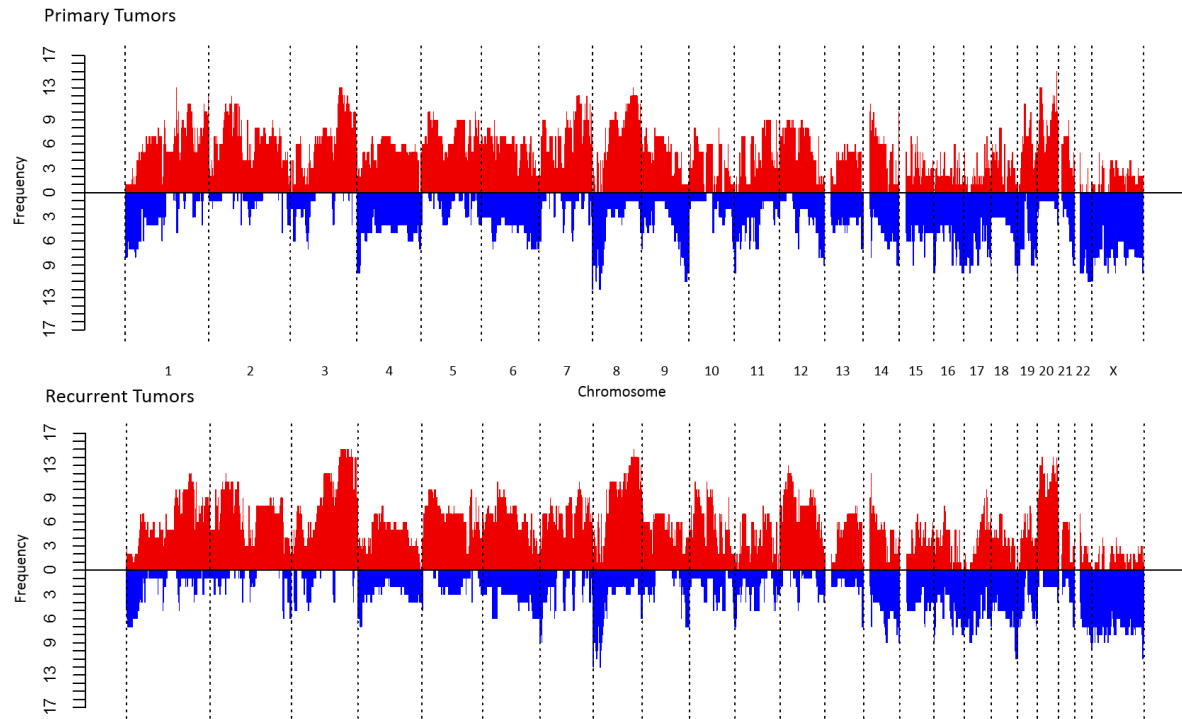


Fig. S5a. Copy number variation profiles among recurrent and their paired primary tumors.

Copy number variations across the genome for 17 paired primary and recurrent samples. Copy number variations were de-noised and segmented with a CBS algorithm. Segments with CNVs were plotted across the entire genome (red= gain; blue= loss).

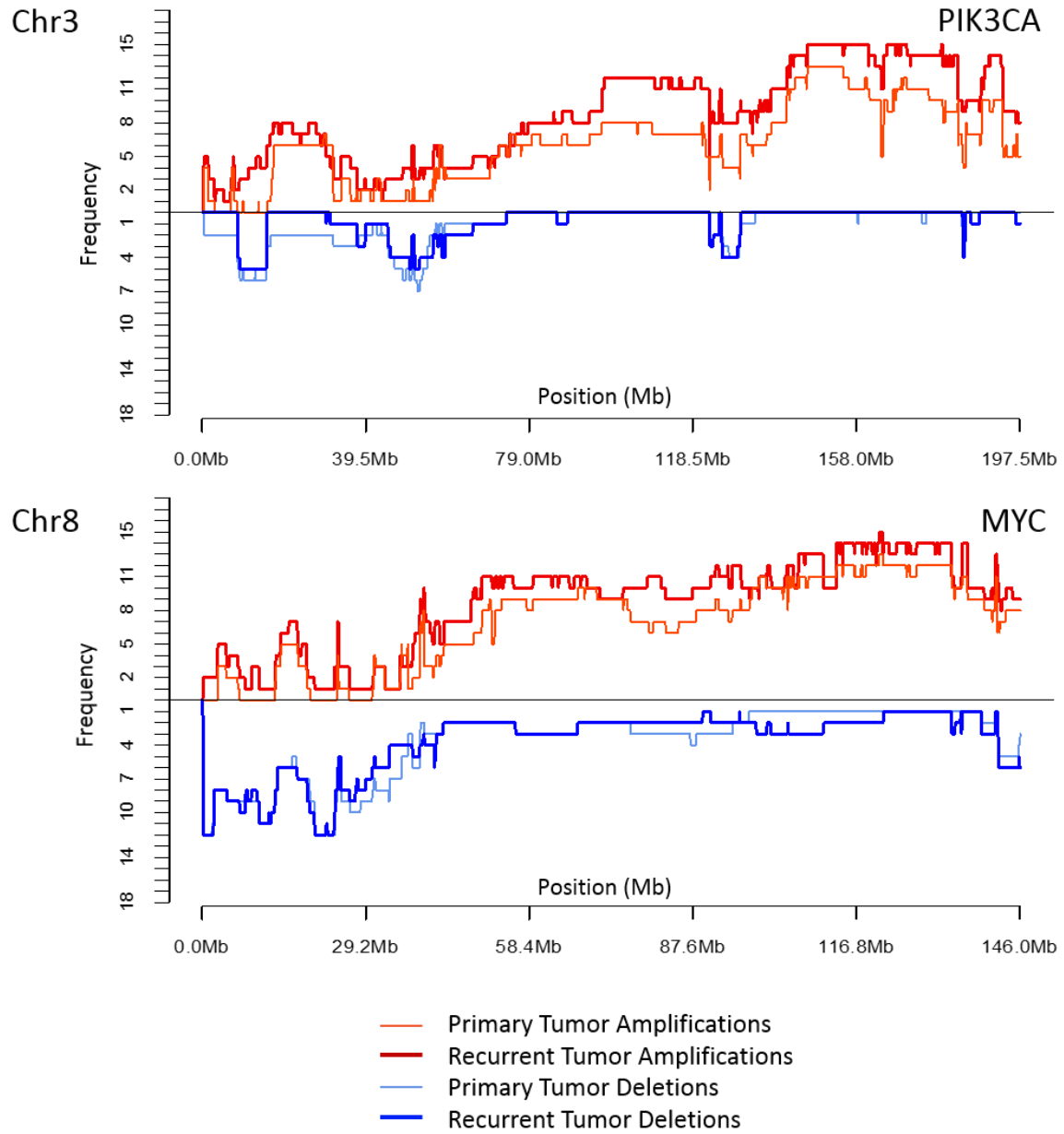


Fig. S5b. Chromosome copy number variation profiles for recurrent and paired primary samples. Detailed copy number variation profiles for recurrent and paired primary samples in Chromosome 3, harboring PIK3CA, and Chromosome 8, harboring C-MYC, are shown.

PIK3CA

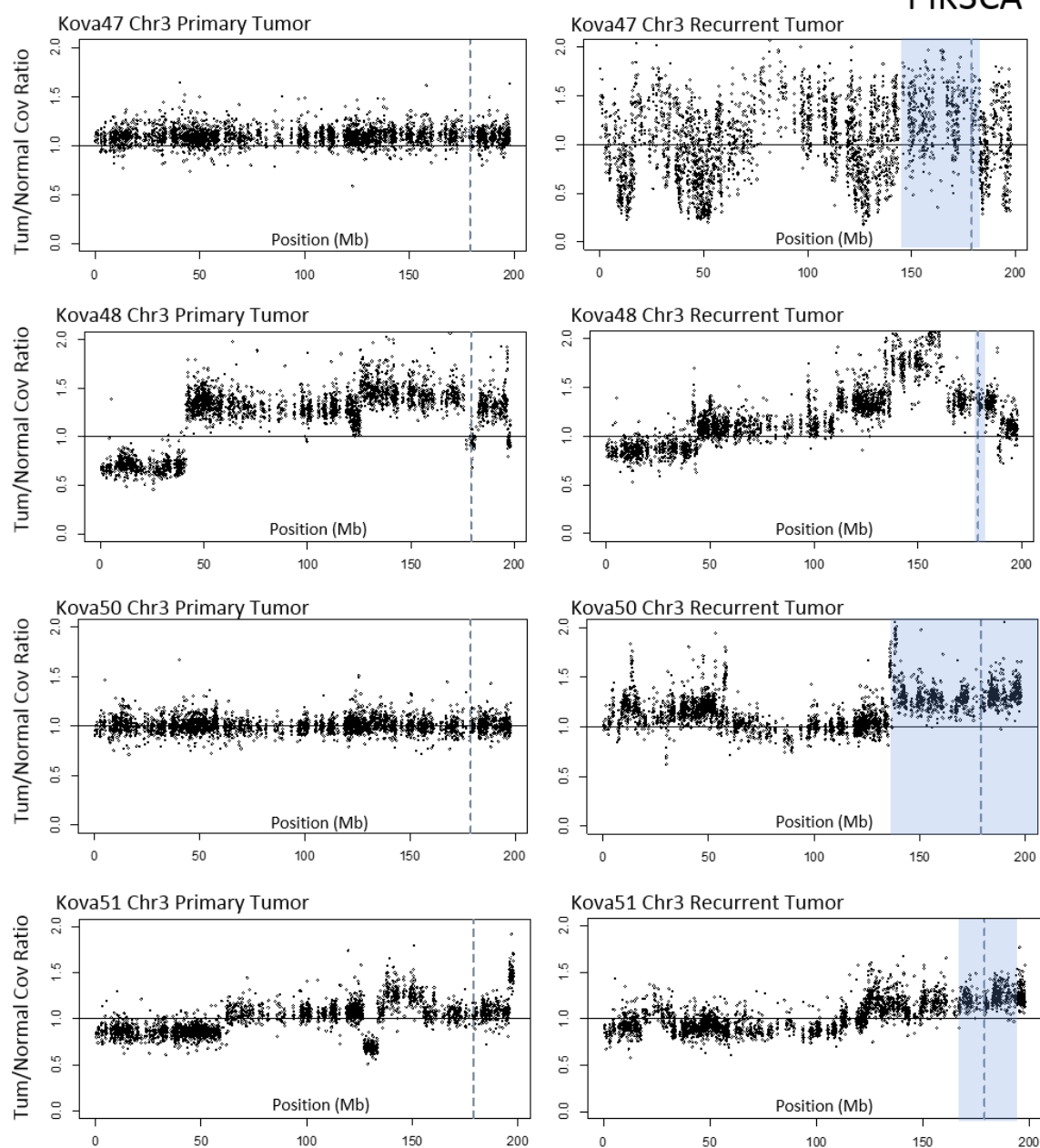


Fig. S5c. Coverage Ratio in CNV Gains in Recurrence. Tumor/Normal Coverage ratios were analyzed across chromosomes 3, covering PIK3CA amplifications in patients with called CNV gains in recurrence. Coverage ratios were normalized to mean coverage depth of each exome.

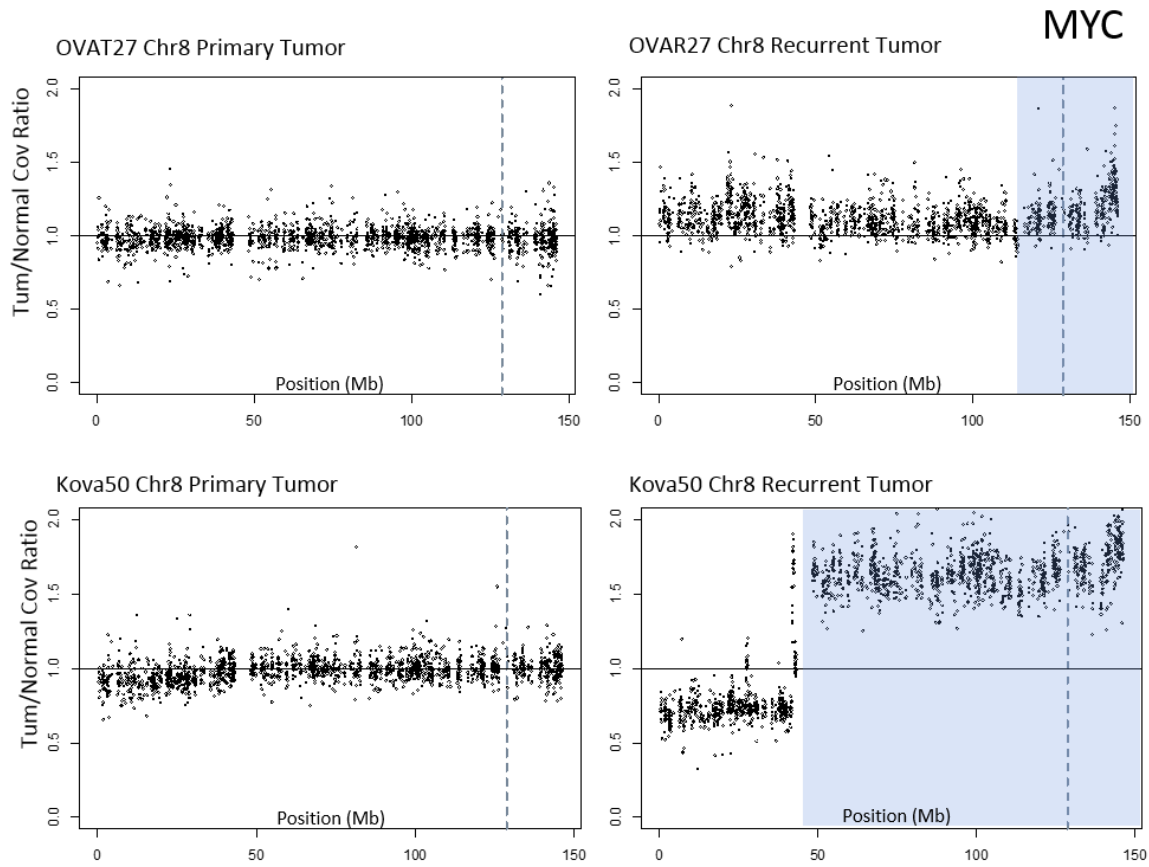


Fig. S5d. Coverage Ratio in CNV Gains in Recurrence. Tumor/Normal Coverage ratios were analyzed across chromosomes 8 covering MYC amplifications in patients with called CNV gains in recurrence. Coverage ratios were normalized to mean coverage depth of each exome.

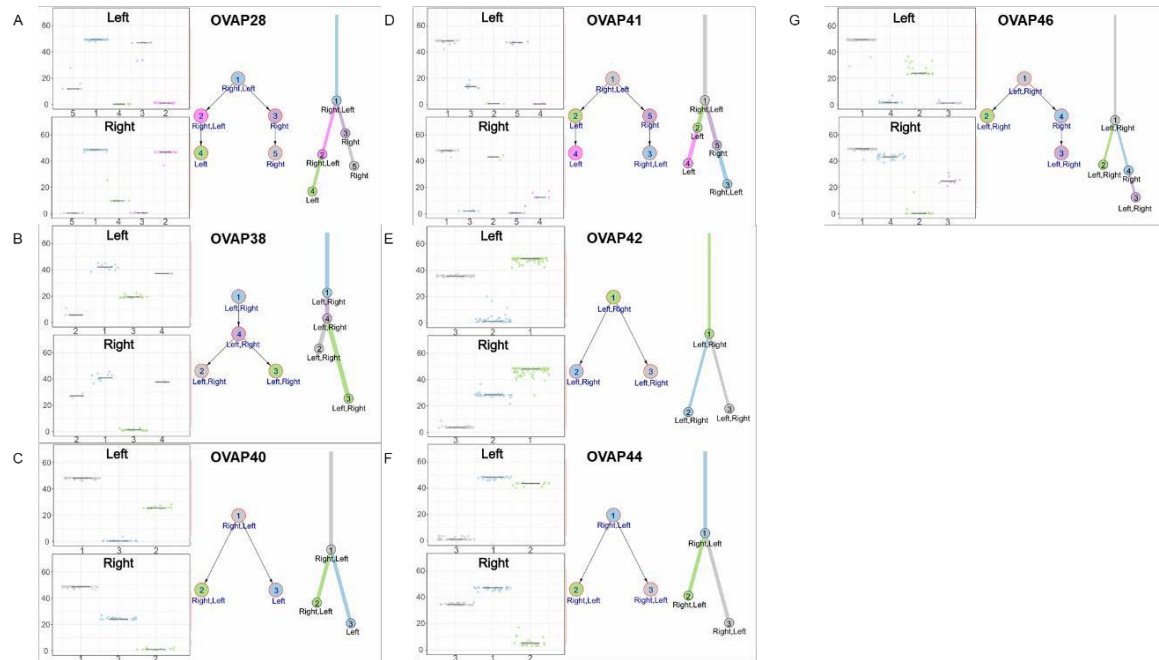


Fig. S6. Clustering of subclones and clonal evolution inference in SBOC. (A-G) Left: clusters of variants based on the variant allele fraction (VAF) in left and right ovarian tumors. Points represent the VAFs of each variant in each cluster. Middle: node-based clonal evolution trees. Right: branch-based clonal evolution trees. Branch lengths represent the number of somatic variants in the clusters.

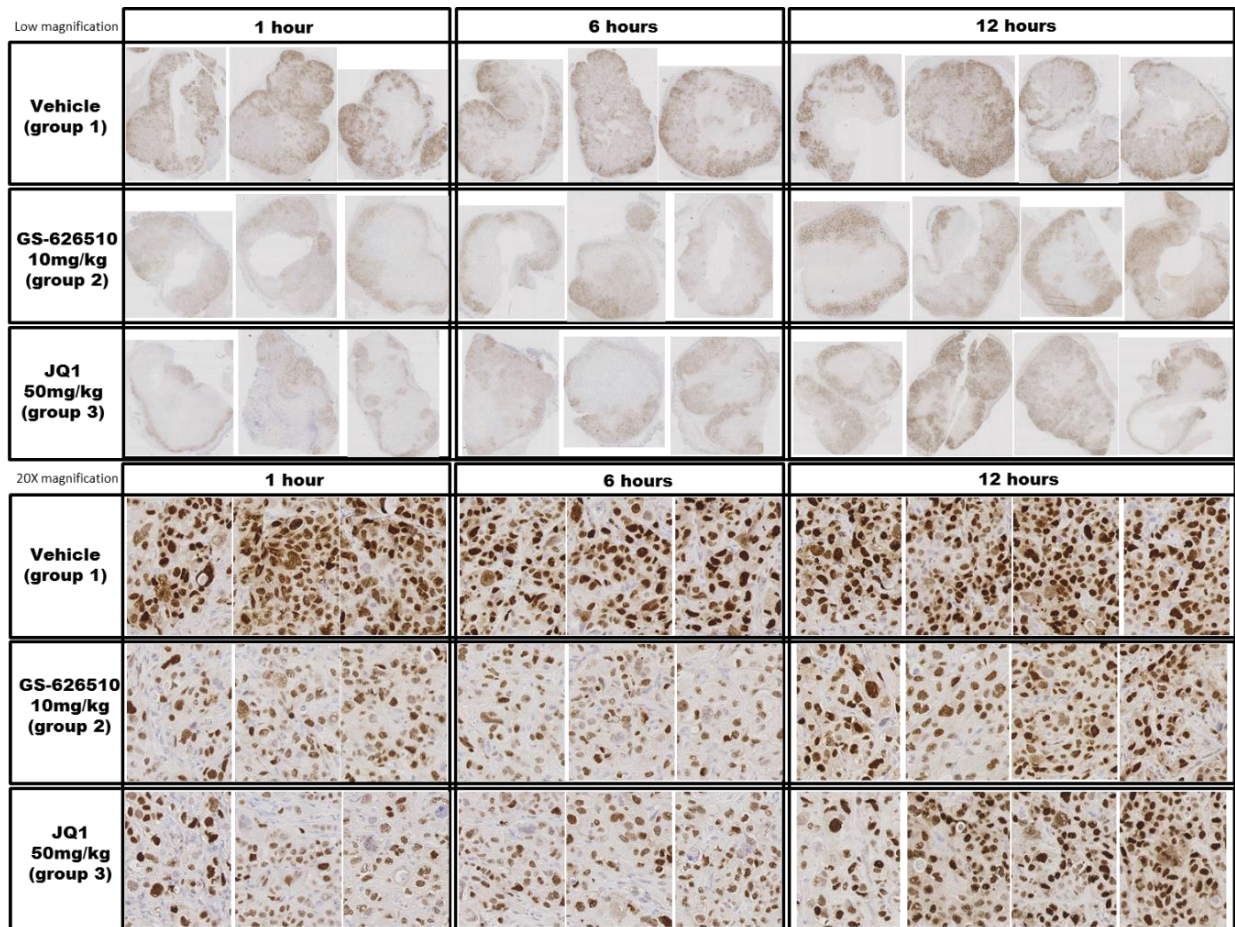









Fig. S7. Ex vivo c-Myc expression assessed by IHC on the OSC-KRCH31 xenograft tumor samples, excised 1 hour, 6 hours and 12 hours after the last dose of GS-626510 at 10 mg/kg, JQ1 at 50 mg/kg and vehicle for oral gavage studies, following 21 days of treatment.

Table S1. Clinical features of primary, metastatic and recurrent ovarian cancer samples (n=90) used for WES and primary cell lines and xenografts used for in vitro and in vivo experiments with GS-626510.

kova 1-ovaM_1	OSPC	IIIC	G3	W
kova 2-ovaM_2	OSPC	IIIC	G3	W
kova 3- ovaM_3	OSPC	IIIC	G3	W
kova 4- ovaM_4	OSPC	IIIC	G3	W
kova 5- ovaM_5	CC	IV	G3	W
kova 6- ovaM_6	OSPC	IIIC	G3	W
kova 7- ovaM_7	OSPC	IIIC	G3	W
kova 8- ovaM_8	OSPC EAC*	IIIC	G3	W
kova 9- ovaM_9	OSPC	IIIC	G3	W
kova 10- ovaM_10	OSPC	IIIC	G3	W
kova 11-ovaM_11	OSPC	IIIC	G3	W
kova 12-ovaM_12	OSPC	IIIC	G3	W
kova 13- ova_M13	OSPC	IIIC	G3	W
kova 15- ovaM_15	OSPC	IIIB	G2	W
kova 16- ovaM_16	OSPC EAC*	IIIC	G3	W
kova 17-ovaM_17	OSPC	IIIA	G2	W
kova 18-ovaM_18	OSPC	IIIC	G3	W
kova 19-ovaM_19	EAC	IIIC	G3	W
kova 20-ovaM_20	OSPC	IV	G3	W
kova 21-ovaM_21	ACA	IV	G3	W
kova 22-ovaM_22	OSPC	IV	G3	W
kova 23-ovaM_23	ACA	IIIC	G3	W
kova 24-ovaM_24	OSPC	IIIC	G3	W
kova 25-ovaM_25	OSPC	IV	G3	W
kova 26-ovaM_26	OSPC	IV	G3	W
kova 27-ovaM_27	OSPC	IIIC	G3	W
kova 29-ovaM_29	OSPC	IIIC	G3	W
kova 30-ovaM_30	OSPC	IIIC	G3	W
kova 31-ovaM_31	CC	IIIC	G3	W
kova 32-ovaM_32	OSPC	IV	G2	W
kova 33-ovaM_33	OSPC	IIIC	G3	W
kova 34-ovaM_34	EAC	IV	G3	W
kova 35-ovaM_35	EAC	IIIC	G3	W
kova 28L-R	OSPC	IIIC	G3	W
kova 36L-R	OSPC	IIIC	G3	W
kova 37L-R	EAC	IIIA	G2	W
kova 38L-R	OSPC	IIIC	G3	W
kova 39L-R	EAC	IIC	G3	W

	primary and meta
	primary L/R
	primary, recurrent
	primary, recurrent and meta
	primary L/R, recurrent
	Primary Only
	meta

*MIXED

OSPC	serous papillary	71%
CC	clear cell	6,5%
EAC	Endometrioid	6,5%
ACA	Dedifferentiated	2,6%
MIXED	Mixed histology	13%

Percentages may not sum to 100 due to rounding

kova 40L-R	OSPC EAC*	IIC	G3	W
kova 41L-R	OSPC EAC*	IIIC	G3	W
kova 42L-R	OSPC	IIC	G3	W
kova 43L-R	OSPC	IIIC	G3	W
kova 44L-R	OSPC EAC*	IIIC	G3	W
kova 45L-R	OSPC	IIIC	G2	W
kova 46L-R	OSPC	IIIC	G3	W
kova 47-ovaR_47	OSPC	IIIC	G2	W
kova 48-ovaR_48	OSPC	IIIC	G3	W
kova 49-ovaR_49	OSPC	III	G3	W
kova 50-ovaR_50	CC	IIC	G3	W
kova 51-ovaR_51	OSPC	IIIC	G3	W
kova 52-ovaM_52-ova_R52	OSPC	III	G3	W
kova 53L-R- ovaR-53	CC EAC*	IIIC	G3	W
kova 54-ovaR_54	OSPC	IV	G3	W
kova 55-ovaM 55-ova_R55	OSPC	IIIC	G3	W
kova 56-ovaR_56	CC	IIIC	G3	W
kova 57-ovaR_57	OSPC	IIIC	G3	W
kova 58-ovaR_58	OSPC	IIB	G3	W
kova 59-ovaR_59	OSPC	IIIC	G3	W
kova 60-ovaR_60	OSPC	IIIC	G3	W
OVAT1-OVAM1	OSPC	IIIC	G3	W
OVAT2-OVAM2	OSPC	IIIB	G3	W
OVAT3-OVAM3	OSPC	IIIC	G3	W
OVAT4	OSPC	IV	G3	W
OVAT5-OVAM5	OSPC	IIIC	G3	W
OVAT6-OVAM6	OSPC	IIIC	G3	W
OVAT7	OSPC	IIIC	G3	W
OVAT8	OSPC	IIIC	G3	W
OVAT9	OSPC CC*	IIIC	G3	W
OVAT10	OSPC EAC*	IIIA	G3	W
OVAT11	OSPC CC EAC*	IIIC	G3	H
OVAT12-OVAR12	OSPC CC*	IIIC	G3	W
OVAT25	OSPC	IV	G3	W
OVAT26-OVAM26	OSPC	IV	G3	O
OVAT27-OVAR27	OSPC	IIC	G3	W
OVAT29	OSPC	IIIC	G3	W

Cell lines

PATIENT CODE	HISTOLOGY	STAGE	GRADE	RACE
OVA10	CC	IIC	G3	W
OSC-KRCH31	OSPC	IV	G3	W

PDX

PATIENT CODE	HISTOLOGY	STAGE	GRADE	RACE
OSC-OMM78	OSPC	IIIC	G3	W

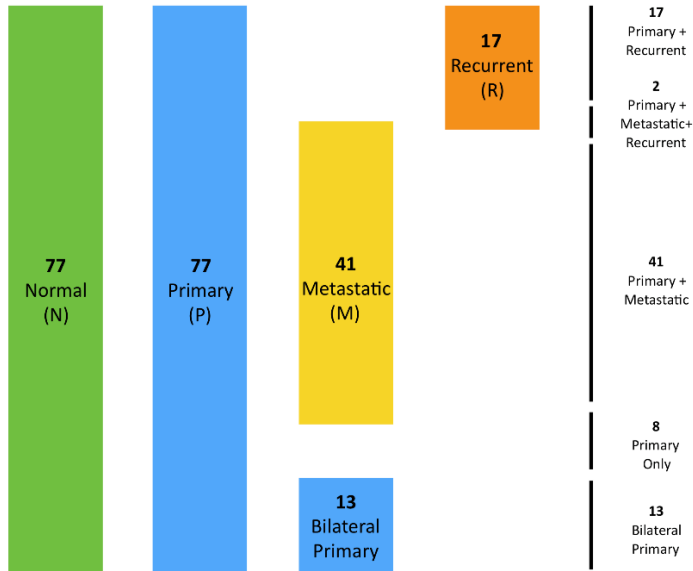


Table S2. Sequencing metrics for tumor samples and matched normal samples. *One primary sample was excluded from the final analysis secondary to low purity.

Tumor Type	Normal	Primary	Metastatic	Recurrent
Number	77	91*	41	17
Read length:	74	74	74	74
Reads per lane:	100	191	205	189
Mean coverage:	101	186	197	183
Median coverage:	85	152	164	146
% Reads on-target:	70.90	68.82	68.19	68.24
% Bases on-target:	60.07	58.25	57.65	57.69
% of bases covered at least 4x	97.72	98.28	98.23	98.21
% of bases covered at least 10x	95.56	96.96	96.84	96.67
% of bases covered at least 20x	91.06	94.58	94.42	93.83
Mean error rate:	29.74%	39.30%	39.71%	35.88%
PCR duplicates (%):	4.88	6.08	6.86	5.32

Table S3. TP53 Somatic Mutations in Primary Tumors

Histology	PatientID	Position	Ref>Alt	AACChange	MutationType	RefReads	NonRefReads
EAC	kova35	7578406	C>T	R43H	nonsynonymous SNV	9	45
EAC	kova34	7578190	T>C	Y88C	nonsynonymous SNV	61	178
OSPC	kova49	7577022	G>A	R174X	stopgain	125	41
ACA	kova23	7577570	C>T	M105I	nonsynonymous SNV	189	44
OSPC	kova42	7579542	CGTCCGGGGACAGCATCAA>-	L4fs	frameshift deletion	53	37
OSPC	kova46	7576852	C>T	NA	splicing	100	71
OSPC	kova22	7577536	T>A	R117W	nonsynonymous SNV	59	102
OSPC	ovat5	7578210	TCGAAAAGTGTT>-	78_81del	nonframeshift deletion	119	126
OSPC	kova30	7579528	C>T	W14X	stopgain	6	61
OSPC	kova26	7579369	G>C	S67R	nonsynonymous SNV	29	44
OSPC	kova59	7577121	G>A	R141C	nonsynonymous SNV	37	108
OSPC EAC	kova16	7578236	A>G	Y73H	nonsynonymous SNV	53	125
OSPC	kova20	7577124	C>A	V140L	nonsynonymous SNV	63	76
OSPC EAC	ovat10	7574030	G>-	R201fs	frameshift deletion	67	16
OSPC	kova13	7577100	T>C	R148G	nonsynonymous SNV	63	135
OSPC	kova48	7574021	C>-	E204fs	frameshift deletion	4	52
OSPC	kova2	7579368	A>-	Y68fs	frameshift deletion	23	36
OSPC	kova58	7578550	G>A	S88F	nonsynonymous SNV	16	99
OSPC	kova27	7578406	C>T	R43H	nonsynonymous SNV	6	50
OSPC EAC	kova8	7578541	A>T	L91H	nonsynonymous SNV	8	68
OSPC	kova12	7578271	TGC>-	60_61del	nonframeshift deletion	29	118
OSPC	kova12	7578273	->AA	Q60fs	frameshift insertion	28	118
OSPC	ovat2	7577551	C>A	G112C	nonsynonymous SNV	78	73
CC	kova31	7578211	C>A	R81L	nonsynonymous SNV	104	188
OSPC EAC	kova44	7577574	T>C	Y104C	nonsynonymous SNV	29	192
OSPC	kova57	7577539	G>A	R116W	nonsynonymous SNV	30	79
OSPC	kova11	7578535	T>C	K93R	nonsynonymous SNV	10	8
OSPC	Kova1	7579349	A>C	F74C	nonsynonymous SNV	11	61
OSPC EAC	kova40	7578449	C>T	A29T	nonsynonymous SNV	6	46
OSPC	kova9	7579316	->A	C85fs	frameshift insertion	16	32
OSPC	kova25	7578535	T>C	K93R	nonsynonymous SNV	17	63
ACA	kova21	7577106	G>C	P146A	nonsynonymous SNV	2	141
OSPC	kova28	7578535	T>C	K93R	nonsynonymous SNV	10	96
OSPC	ovat6	7577018	C>A	NA	splicing	112	37
OSPC	kova15	7577121	G>T	R141S	nonsynonymous SNV	81	75
OSPC	kova45	7577082	C>-	E154fs	frameshift deletion	21	104
EAC	kova19	7578427	T>C	H36R	nonsynonymous SNV	41	11
OSPC	kova54	7578188	C>A	E89X	stopgain	159	153
OSPC	kova6	7578442	T>C	Y31C	nonsynonymous SNV	11	36

OSPC CC	ovat12	7574012	C>A	E207X	stopgain	28	35
OSPC	ovat8	7578483	G>-	S17fs	frameshift deletion	86	43
CC	kova5	7577099	C>G	R148T	nonsynonymous SNV	79	89
OSPC	kova52	7578370	C>G	NA	splicing	49	9
OSPC	kova10	7578382	G>C	S51X	stopgain	15	37
OSPC	ovat26	7578291	T>C	NA	splicing	77	158
OSPC	kova38	7577058	C>A	E162X	stopgain	3	137
OSPC EAC	kova41	7578413	C>T	V41M	nonsynonymous SNV	26	21
OSPC	kova7	7577547	C>A	G113V	nonsynonymous SNV	15	101
EAC	kova39	7578440	T>C	K32E	nonsynonymous SNV	41	42
OSPC	kova3	7578222	TC>-	R77fs	frameshift deletion	111	10
OSPC	Kova36	7577142	C>A	G134X	stopgain	107	49
OSPC	kova33	7577572	T>C	M105V	nonsynonymous SNV	170	50
OSPC	kova33	7578190	T>C	Y88C	nonsynonymous SNV	263	112
OSPC	kova55	7577574	T>C	Y104C	nonsynonymous SNV	26	38
OSPC	ovat27	7578271	T>C	H61R	nonsynonymous SNV	191	27
OSPC	kova17	7578203	C>A	V84L	nonsynonymous SNV	13	218
OSPC	kova4	7577538	C>T	R116Q	nonsynonymous SNV	13	155
OSPC	kova18	7578406	C>T	R43H	nonsynonymous SNV	10	41
OSPC	ovat7	7577120	C>T	R141H	nonsynonymous SNV	63	107
OSPC	kova29	7577120	C>T	R141H	nonsynonymous SNV	44	174
OSPC	kova51	7577120	C>T	R141H	nonsynonymous SNV	41	65
OSPC CC	ovat9	7577538	C>T	R116Q	nonsynonymous SNV	90	42
OSPC	kova24	7577094	G>A	R150W	nonsynonymous SNV	167	31
OSPC	kova60	7577120	C>T	R141H	nonsynonymous SNV	57	62
OSPC	ovat3	7578212	G>A	R81X	nonsynonymous SNV	90	148
OSPC	ovat4	7577094	G>A	R150W	nonsynonymous SNV	17	84
OSPC	ovat1	7578206	T>C	S83G	nonsynonymous SNV	34	244
OSPC	ovat29	7579480	G>-	A69fs	frameshift deletion	86	18

Table S4. Mismatch repair mutations. Tumors with mismatch repair gene mutations contained significantly higher somatic mutation burdens than tumors without mismatch repair gene mutations.

Primary		
TumorID	Somatic Mutations	Mutated Gene
Kova53-Left	1267	MSH2(x2), MSH3, PMS1
Kova53-Right	263	MSH2, PMS1
Kova35	108	MLH1
OVAT6	57	MLH3
Kova16	98	MLH3
Kova1	70	MSH3
Kova34	160	MSH3
Kova31	80	PMS1
Metastatic		
TumorID	Somatic Mutations	Mutated Gene
Kova16	99	MLH3
OVAT6	76	MLH3
Kova34	147	MSH3
Kova31	79	PMS1

Table S5. PIK3CA mutations. Pathogenic mutations indicate evidence of clinical pathogenicity. “Known Gain of Function” mutations have been functionally characterized as oncogenic gain of function in previously published *in vitro* studies.

Patient	Mutation	Deleteriousness
Primary	6.5% (5/77 Patients)	
Kova5	E542K	Pathogenic
OVAT8	N345K	Known Gain of Function
Kova37-Right	C420R	Known Gain of Function
Kova37-Right+Left	G106V	Known Gain of Function
Kova53-Left	R93Q	Known Gain of Function
Kova53-Left	V334M	
Kova56	H1047R	Pathogenic
Metastatic	4.9% (2/41 Patients)	
Kova5	E542K	Pathogenic
OVAT8	N345K	Known Gain of Function
Recurrent	17.6% (3/17 Patients)	
Kova50	E545K	Pathogenic
Kova53	R93Q	Known Gain of Function
Kova53	H1047R	Pathogenic
Kova53	V334M	
Kova56	H1047R	Pathogenic

Table S6a. Key recurrent CNVs. The most significant recurrent CNVs, as found by the GISTIC algorithm, were compared in primary, metastatic, and recurrent settings for relative prevalence. Putative genes for each CNV were determined based on cancer genes found within the recurrently mutated regions as well as known associations between CNVs and driver genes.

Putative Gene	Location	Primary (n=77)	Affected	Metastatic (n=41)	Affected	Recurrent (n=17)	Affected
Amplifications							
PIK3CA	3q26.1	53	68.83%	29	70.73%	15	88.24%
MYC	8q24.3	57	74.03%	32	78.05%	14	82.35%
	14q11.2	44	57.14%	25	60.98%	12	70.59%
Deletions							
RPI22, ARID1A	1p36	41	53.25%	24	58.54%	9	52.94%
VHL	3p25.3	35	45.45%	20	48.78%	8	47.06%
FGFR3 CRIPAK	4p16.1	39	50.65%	24	58.54%	8	47.06%
CARD11	7p22.3	41	53.25%	31	75.61%	9	52.94%
EGR3	8p21	52	67.53%	27	65.85%	14	82.35%
NOTCH1	9q34	49	63.64%	27	65.85%	10	58.82%
HRAS	11p15.4	53	68.83%	30	73.17%	11	64.71%
GNA11 STK11	19p13.3	61	79.22%	38	92.68%	10	58.82%

Table S6b. CNV Transmission in Matched Recurrent and Primary Tumors. Amplifications were calculated based on normalized read counts at the PIK3CA and MYC loci in matched pairs of primary and recurrent tumors. Amplifications in recurrent tumors that were not present in their matched primary tumors are indicated in bold.

Patient	PIK3CA Copy Number		MYC Copy Number	
	Primary	Recurrent	Primary	Recurrent
OVAT12	Amplification	Amplification	Amplification	Amplification
OVAT27	Amplification	Amplification		Amplification
OVAT31				
kova_47		Amplification		
kova_48		Amplification	Amplification	Amplification
kova_49	Amplification	Amplification	Amplification	Amplification
kova_50		Amplification		Amplification
kova_51		Amplification	Amplification	Amplification
kova_52	Amplification	Amplification	Amplification	Amplification
kova_53	Amplification	Amplification		
kova_54			Amplification	Amplification
kova_55	Amplification	Amplification	Amplification	Amplification
kova_56	Amplification	Amplification	Amplification	Amplification
kova_57	Amplification	Amplification	Amplification	Amplification
kova_58	Amplification	Amplification	Amplification	Amplification
kova_59	Amplification	Amplification	Amplification	Amplification
kova_60	Amplification	Amplification	Amplification	Amplification

Table S6c. Genes within key amplification regions. Amplification boundaries were determined based on the region of amplification in recurrent samples. Genes in the region were counted and cross-referenced with known cancer genes.

Amplification	Start	End	Genes in Region	Cancer Genes
3q26	142060002	178959999	282	ATR, MECOM, TBL1XR1, PIK3CA
8q23-24	105620001	139619999	178	RAD21, MYC
14q11	22380001	22960000	60	

Table S7. Mutation transmission statistics.

Primary to Metastatic Transmission (n=41)						
	Somatic Mutations in all genes			Somatic Mutations in known cancer genes		
	Primary specific	Transmitted	Metastatic specific	Primary specific	Transmitted	Metastatic specific
MEAN	36.98	54.32	19.44	0.68	2.27	0.27
TOTAL	1516	2227	797	28	93	11
%	40.50%	59.50%		23.14%	76.86%	

Primary to Recurrent Transmission (n=16)						
	Somatic Mutations in all genes			Somatic Mutations in known cancer genes		
	Primary specific	Transmitted	Recurrent specific	Primary specific	Transmitted	Recurrent specific
MEAN	35.25	42.06	49.75	0.44	1.81	0.75
TOTAL	564	673	796	7	29	12
%	45.59%	54.41%		19.44%	80.56%	

Metastatic to Recurrent Transmission (n=2)						
	Somatic Mutations in all genes			Somatic Mutations in known cancer genes		
	Metastatic specific	Transmitted	Recurrent specific	Metastatic specific	Transmitted	Recurrent specific
MEAN	6.5	32	36.5	0	1	0.5
TOTAL	13	64	73	0	2	1
%	16.88%	83.12%		0.00%	100.00%	

Table S8a. Pathogenic germline mutations in homologous recombination repair genes. somatic and pathogenic germline variants were analyzed together to estimate the prevalence of homologous recombination repair deficiency. 25% of patients contained either a pathogenic germline mutation or somatic mutation in a homologous recombination repair gene.

SampleID	GeneID	Chrom.	Position	Ref>NonRef	AAChange	SVMscore	SVMpred.	ClinvarAnno
OVAN5	BRCA1	17	41243844	TTTAC>-	V1187fs	NA	NA	pathogenic
OVAN6	BRCA1	17	41276045	CT>-	E23fs	NA	NA	pathogenic
kova12CTRneg	BRCA1	17	41209079	->G	Q1709fs	NA	NA	pathogenic
kova26CTRneg	BRCA1	17	41258504	A>C	C61G	0.951	D	pathogenic
kova29CTRneg	BRCA1	17	41243800	C>A	E1250X	.	.	pathogenic
kova34CTRneg	BRCA1	17	41258504	A>C	C61G	0.951	D	pathogenic
kova3CTRneg	BRCA1	17	41245179	GT>-	T743fs	NA	NA	pathogenic
kova44CTRneg	BRCA1	17	41258495	A>G	C64R	0.96	D	pathogenic
kova51CTRneg	BRCA1	17	41243800	C>A	E1250X	.	.	pathogenic
kova9CTRneg	BRCA1	17	41258495	A>G	C64R	0.96	D	pathogenic
kova20CTRneg	BRCA2	13	32911538	G>T	E1016X	.	.	pathogenic
kova24CTRneg	BRCA2	13	32911240	T>-	C916fs	NA	NA	pathogenic
kova30CTRneg	BRCA2	13	32929170	A>T	R2394X	.	.	pathogenic
kova4CTRneg	BRCA2	13	32910537	TC>-	I682fs	NA	NA	pathogenic
kova8CTRneg	BRCA2	13	32929170	A>T	R2394X	.	.	pathogenic
OVAN9	BRCA2	13	32914759	G>-	E2089fs	NA	NA	
OVAN9	BRCA2	13	32914761	A>-	H2090fs	NA	NA	
kova595CTRneg	CHEK2	22	29095917	C>G	G306A	0.988	D	pathogenic
kova41CTRneg	PALB2	16	23646550	C>-	G439fs	NA	NA	pathogenic
kova57CTRneg	BRIP1	17	59937223	G>C	P47A	0.013	D	pathogenic

Table S8b. Somatic mutations in homologous recombination repair genes.

PairedNormal	SampleID	Chr	Start	End	Ref	Alt	GeneID	MutationType
Primary Tumors								
kova54CTRneg	OVAP_54	17	41247884	41247884	T	-	BRCA1	frameshift deletion
kova18CTRneg	OVAP_18	16	23634433	23634433	A	G	PALB2	synonymous SNV
kova30CTRneg	OVAP_30	16	23619254	23619254	A	C	PALB2	nonsynonymous SNV
kova51CTRneg	OVAP_51	11	108139207	108139207	C	T	ATM	synonymous SNV
kova35CTRneg	OVAP_35	13	32969071	32969071	G	A	BRCA2	splicing
kova22CTRneg	OVAP_22	13	32912843	32912843	G	-	BRCA2	frameshift deletion
kova29CTRneg	OVAP_29	13	32911403	32911403	T	G	BRCA2	nonsynonymous SNV
kova58CTRneg	OVAP_58	13	32910494	32910494	A	G	BRCA2	nonsynonymous SNV
kova6CTRneg	OVAP_6	13	32912240	32912240	G	T	BRCA2	stopgain
kova44CTRneg	OVAP_44_1	8	90993102	90993103	CC	-	NBN	frameshift deletion
kova50CTRneg	OVAP_50	3	142231226	142231226	G	C	ATR	synonymous SNV
kova4CTRneg	OVAP_4	3	142281468	142281468	C	A	ATR	nonsynonymous SNV
kova21CTRneg	OVAP_21	3	142285057	142285057	C	T	ATR	synonymous SNV
Metastatic Tumors								
kova18CTRneg	OVAM_18	16	23634433	23634433	A	G	PALB2	synonymous SNV
kova30CTRneg	OVAM_30	16	23619254	23619254	A	C	PALB2	nonsynonymous SNV
kova22CTRneg	OVAM_22	13	32912843	32912843	G	-	BRCA2	frameshift deletion
kova35CTRneg	OVAM_35	13	32969071	32969071	G	A	BRCA2	splicing
kova6CTRneg	OVAM_6	13	32912240	32912240	G	T	BRCA2	stopgain
kova4CTRneg	OVAM_4	3	142281468	142281468	C	A	ATR	nonsynonymous SNV
kova21CTRneg	OVAM_21	3	142285057	142285057	C	T	ATR	synonymous SNV
Recurrent Tumors								
kova54CTRneg	OVAR_54	17	41247884	41247884	T	-	BRCA1	frameshift deletion
kova58CTRneg	OVAR_58	13	32910494	32910494	A	G	BRCA2	nonsynonymous SNV

Table S8c. All rare germline mutations in homologous recombination repair genes.

SampleID	GeneID	Chrom.	Position	Ref>NonRef	AAChange	SVMScore	SVMPred.
OVAN11	BRCA1	17	41245825	C>A	E575X	.	.
OVAN25	BRCA1	17	41244757	C>A	V931L	-0.663	T
OVAN5	BRCA1	17	41243843	GTTTAC>G	V1234fs	.	.
OVAN6	BRCA1	17	41276044	ACT>A	E23fs	.	.
kova12CTRneg	BRCA1	17	41209079	T>TG	Q1777fs	.	.
kova26CTRneg	BRCA1	17	41258504	A>C	C61G	0.951	D
kova28CTRneg	BRCA1	17	41244964	T>C	K862E	0.15	D
kova29CTRneg	BRCA1	17	41243800	C>A	E1250X	.	.
kova34CTRneg	BRCA1	17	41258504	A>C	C61G	0.951	D
kova3CTRneg	BRCA1	17	41245178	AGT>A	T790fs	.	.
kova41CTRneg	BRCA1	17	41244658	C>T	G964R	-0.063	T
kova44CTRneg	BRCA1	17	41258495	A>G	C64R	0.96	D
kova51CTRneg	BRCA1	17	41243800	C>A	E1250X	.	.
kova9CTRneg	BRCA1	17	41258495	A>G	C64R	0.96	D
OVAN10	BRCA2	13	32913077	G>A	G1529R	0.601	D
OVAN9	BRCA2	13	32914758	AG>A	E2089fs	.	.
OVAN9	BRCA2	13	32914760	CA>C	H2090fs	.	.
kova20CTRneg	BRCA2	13	32911538	G>T	E1016X	.	.
kova20CTRneg	BRCA2	13	32911751	A>T	T1087S	-0.927	T
kova24CTRneg	BRCA2	13	32911239	GT>G	C916fs	.	.
kova30CTRneg	BRCA2	13	32929170	A>T	R2394X	.	.
kova4CTRneg	BRCA2	13	32910536	ATC>A	I682fs	.	.
kova8CTRneg	BRCA2	13	32929170	A>T	R2394X	.	.
kova32CTRneg	BARD1	2	215609826	C>T	G623E	-0.392	T
kova58CTRneg	BARD1	2	215645430	G>C	L390V	-0.837	T
kova595CTRneg	CHEK2	22	29095917	C>G	G85A	0.988	D
OVAN27	PALB2	16	23635348	A>C	L939W	-0.715	T
kova19CTRneg	PALB2	16	23634417	T>G	K957Q	-1.001	T
kova41CTRneg	PALB2	16	23646549	AC>A	G439fs	.	.
OVAN11	ATM	11	108224537	G>A	V2906I	0.141	D
kova16CTRneg	ATM	11	108160454	A>C	K1454N	-0.564	T
kova39CTRneg	ATM	11	108190686	A>T	E2118V	-0.941	T
kova55CTRneg	ATM	11	108121667	T>C	F492S	-0.716	T
OVAN10	BRCA2	13	32913077	G>A	G1529R	0.601	D
OVAN9	BRCA2	13	32914758	AG>A	E2089fs	.	.
OVAN9	BRCA2	13	32914760	CA>C	H2090fs	.	.
kova20CTRneg	BRCA2	13	32911538	G>T	E1016X	.	.

kova20CTRneg	BRCA2	13	32911751	A>T	T1087S	-0.927	T
kova24CTRneg	BRCA2	13	32911239	GT>G	C916fs	.	.
kova30CTRneg	BRCA2	13	32929170	A>T	R2394X	.	.
kova4CTRneg	BRCA2	13	32910536	ATC>A	I682fs	.	.
kova8CTRneg	BRCA2	13	32929170	A>T	R2394X	.	.
OVAN2	BRIP1	17	59886102	G>A	S215F	-0.388	T
kova57CTRneg	BRIP1	17	59937223	G>C	P47A	0.013	D
kova2CTRneg	RAD51C	17	56809861	A>G	K328E	0.037	D
kova31CTRneg	RAD51C	17	56770093	C>T	A30V	-0.625	T
kova7CTRneg	CHEK1	11	125503091	C>T	T153I	-0.951	T

Table S9. Damaging BROCA mutations. 36% (28/77) of patients contained a known pathogenic variant as found in CLINVAR, a MetaSVM (Noted as “SVM” in table) damaging mutation, or an indel mutation in a BROCA gene.

SampleID	GeneID	Chrom.	Position	Ref>NonRef	AChange	SVMscore	SVMpred.	ClinvarAnno
OVAN10	MSH2	2	47635690	A>G	Y55C	0.216	D	unknown
OVAN10	RECQL	12	21639483	A>G	M144T	0.678	D	.
OVAN11	ATM	11	108224537	G>A	V2906I	0.141	D	unknown
OVAN11	TP53	17	7577548	C>T	G206S	0.902	D	pathogenic
OVAN1	PTCH1	9	98215833	C>T	V975I	0.237	D	unknown
OVAN5	BRCA1	17	41243843	GTTTAC>G	V1234fs	.	.	pathogenic
OVAN6	NTHL1	16	2096209	G>A	R100C	0.727	D	.
OVAN6	BRCA1	17	41276044	ACT>A	E23fs	.	.	pathogenic
OVAN8	PTCH1	9	98270592	TGCC>T	17_17del	.	.	.
OVAN9	BRCA2	13	32914758	AG>A	E2089fs	.	.	.
OVAN9	BRCA2	13	32914760	CA>C	H2090fs	.	.	.
kova12CTRneg	BRCA1	17	41209079	T>TG	Q1777fs	.	.	pathogenic
kova22CTRneg	RET	10	43604649	G>A	V412M	0.375	D	.
kova24CTRneg	BRCA2	13	32911239	GT>G	C916fs	.	.	.
kova24CTRneg	NF1	17	29654671	C>T	T1808M	0.146	D	.
kova26CTRneg	BRCA1	17	41258504	A>C	C61G	0.951	D	.
kova29CTRneg	BRCA1	17	41243800	C>A	E1250X	.	.	pathogenic
kova2CTRneg	RAD51C	17	56809861	A>G	K328E	0.037	D	.
kova30CTRneg	BRCA2	13	32929170	A>T	R2394X	.	.	pathogenic
kova34CTRneg	BRCA1	17	41258504	A>C	C61G	0.951	D	.
kova39CTRneg	CTNNA1	5	138266269	C>G	D706E	0.185	D	.
kova3CTRneg	BRCA1	17	41245178	AGT>A	T790fs	.	.	.
kova41CTRneg	MITF	3	70014029	T>C	L382P	0.744	D	.
kova41CTRneg	PALB2	16	23646549	AC>A	G439fs	.	.	.
kova43CTRneg	APC	5	112177310	T>C	Y2007H	0.599	D	.
kova44CTRneg	BRCA1	17	41258495	A>G	C64R	0.96	D	pathogenic
kova48CTRneg	MUTYH	1	45798269	T>C	I195V	0.46	D	unknown
kova4CTRneg	MSH6	2	48026006	A>G	K295R	0.322	D	unknown
kova4CTRneg	BRCA2	13	32910536	ATC>A	I682fs	.	.	unknown
kova51CTRneg	BRCA1	17	41243800	C>A	E1250X	.	.	pathogenic
kova54CTRneg	SLX4	16	3640053	CAAT>C	1195_1195del	.	.	.
kova57CTRneg	BRIP1	17	59937223	G>C	P47A	0.013	D	pathogenic
kova595CTRneg	CHEK2	22	29095917	C>G	G85A	0.988	D	.
kova8CTRneg	BRCA2	13	32929170	A>T	R2394X	.	.	pathogenic
kova9CTRneg	BRCA1	17	41258495	A>G	C64R	0.96	D	pathogenic

Table S10. Average quantitative nuclear histological score associated with ex vivo c-MYC expression assessed by IHC in OSC-KRCH31 xenograft tumor samples, excised 1 hour, 6 hours and 12 hours after the last dose of GS-626510 at 10 mg/kg, JQ1 at 50 mg/kg and vehicle for oral gavage studies, following 21 days of treatment.

Dosing Group	Time of collection after dosing	Avg QN H-score	SD	P-value vs Vehicle
Vehicle	1 hour	117.33	5.86	
GS-626510 10mg/kg	1 hour	76.67	2.08	0.0003
JQ1 50mg/kg	1 hour	72.67	15.50	0.0095
Vehicle	6 hours	110.33	6.81	
GS-626510 10mg/kg	6 hours	82.67	9.71	0.0156
JQ1 50mg/kg	6 hours	79.00	5.00	0.0030
Vehicle	12 hours	114.25	8.50	
GS-626510 10mg/kg	12 hours	103.75	7.85	0.1194
JQ1 50mg/kg	12 hours	105.50	14.62	0.3406

References

1. Choi, M. et al. Genetic diagnosis by whole exome capture and massively parallel DNA sequencing. *Proc. Natl. Acad. Sci.* 106, 19096–19101 (2009).
2. Zhao, S. et al. Landscape of somatic single-nucleotide and copy-number mutations in uterine serous carcinoma. *Proc. Natl. Acad. Sci. U. S. A.* 110, 2916–2921 (2013).
3. Beroukhi, R. et al. Assessing the significance of chromosomal aberrations in cancer: Methodology and application to glioma. *Proc Natl Acad Sci USA* 104: 20007–20012 (2007).
4. Favero, F. et al. Sequenza: allele-specific copy number and mutation profiles from tumor sequencing data. *Ann Oncol.* 26: 64-70 (2015).
5. Roth, A. et al. PyClone: statistical inference of clonal population structure in cancer. *Nat Methods.* Apr;11: 396-8 (2014).
6. Dang HX. et al. ClonEvol: clonal ordering and visualization in cancer sequencing. *Ann Oncol.* 28:3076-3082 (2017).
7. Roque, D. et al. Class III β -tubulin overexpression in ovarian clear cell and serous carcinoma as a marker for poor overall survival after platinum/taxane chemotherapy and sensitivity to patupilone. *Am J Obstet Gynecol* 209:62.e1-9 (2013).
8. Bonazzoli, E. et al. Inhibition of BET bromodomain proteins with GS-5829 and GS-626510 in uterine serous carcinoma, a biologically aggressive variant of endometrial cancer. *Clin Cancer Res.* 24(19):4845-4853 (2018).